Resonances in one and two rows of triangular Josephson junction cells

P. Caputo,* M. V. Fistul,† and A. V. Ustinov
Physikalisches Institut III, Universität Erlangen-Nürnberg, Erwin-Rommel-Strasse 1, D-91058 Erlangen, Germany
(Received 13 November 2000; published 8 May 2001)

We present an experimental and analytical study of resonances in the current-voltage characteristics of single and double row triangular Josephson arrays. The magnetic-field dependences of the voltage positions of the resonances have been measured for various cell inductances and junction critical currents. In double row arrays, we have observed a peculiar resonance, whose voltage position decreases with magnetic field. We derive the spectrum of linear electromagnetic waves propagating in the arrays. In the double row array, the spectrum consists of many branches that differ by the behavior of the Josephson junctions transverse to the bias current direction. The measured magnetic-field dependence of the resonance voltages is mapped to the linear mode spectrum and good agreement between experiments and model is found.

DOI: 10.1103/PhysRevB.63.214510 PACS number(s): 74.50.+r, 03.65.Pm

I. INTRODUCTION

The driven Josephson junction ladders and arrays have recently attracted wide interest due to many fascinating phenomena observed in such systems. They show vortex propagation,[1,2] various current-voltage resonances,[3,4] nonlinear dynamic localized modes,[5,6] and may also be practically useful as high-frequency oscillators.[7,8]

A peculiarity of quasi-two-dimensional arrays, i.e., Josephson ladders, and two-dimensional arrays, is the presence of Josephson junctions in both the longitudinal and transverse directions to the bias current [see sketches in Figs. 1(a)–(c)]. In these systems, the Josephson phase dynamics is more complex than in the rather well studied case of one-dimensional parallel arrays,[1,2] due to the higher degree of freedom appearing from the presence of the junctions transverse to the bias. For example, the spectrum $\omega(q)$ of the linear electromagnetic waves (EW's) propagating in the ladders [Fig. 1(a)] contains *two* branches.[3,4,7] Similar behavior has been extensively studied in vertical stacks of long Josephson junctions (see Ref. 9 and references therein), where the inductive coupling between the junctions leads to the splitting of the dispersion relation. The splitting has been found also in coupled one-dimensional parallel arrays.[10] As we turn to the case of two-dimensional arrays, the number of branches in the spectrum $\omega(q)$ increases. This feature has been recently confirmed by a systematic numerical study on dynamical states in underdamped arrays.[11]

It is well known that, in the presence of a magnetic field, the nonlinear interaction between the Josephson current wave and the excited EW's leads to resonant steps in the current-voltage characteristics of extended Josephson systems.[1,13,14] The measured magnetic-field dependence of the voltages of the resonant steps can be mapped to the spectrum $\omega(q)$ by the relationship

$$V_{\rm res}=\frac{\hbar\omega(q)}{2e}, \quad q=f, \tag{1}$$

where $f=\Phi_{\rm ext}/\Phi_0$ is the magnetic flux threading the cell normalized to the magnetic-flux quantum, and it is referred to as frustration parameter. The spectrum $\omega(q)$ for the Josephson ladder with four junctions per elementary cell [Fig. 1(a)] has been calculated in Ref. 3 in the linear approximation, and a good agreement between the measured magnetic-field dependence of the step voltages and Eqs. (1) was found. This system has a remarkable property that at $f=0.5$ an ''out-of-phase'' state of the currents is formed. As the amplitude of the resonant step reaches a maximum, the direction of the mesh currents flowing in adjacent cells alternate from one cell to another, and the so-called ''checkerboard'' structure of the alternating (ac) currents appears.[4,7] The ac currents compensate each other on the horizontal junctions and the total alternating voltage along the ladder is close to zero. This property is an obvious drawback if one wants to

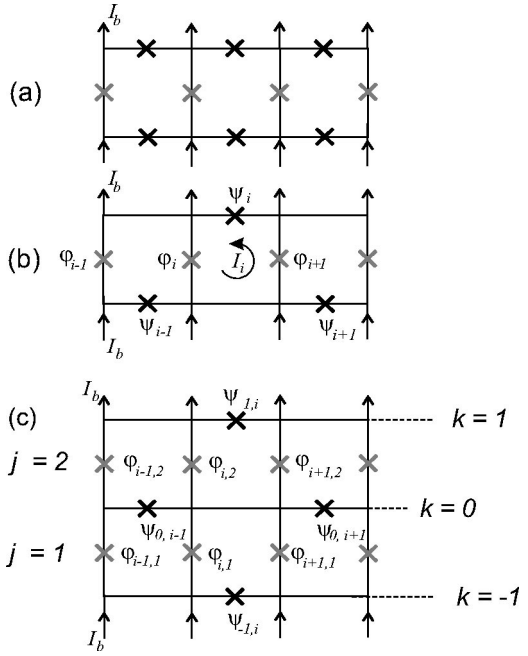

FIG. 1. Sketches of Josephson ladders with (a) four and (b) three Josephson junctions per cell, and of a two-row array (c); $\varphi_{i,j}$ and $\varphi_{i+1,j}$ denote the Josephson phases of the vertical junctions of cell i in row j; $\psi_{i,k}$ denotes the Josephson phases of the horizontal junction of cell i in line k. The magnetic field is applied perpendicular to the plane of the cells and induces a mesh current I_i.

use the ladder as an oscillator. To overcome it, Yukon and Lin proposed[7] to use a *triangular* arrangement of Josephson junctions along the ladder [Figs. 1(b) and (c)]. In this case, at $f=0.5$ an ''in-phase'' state with all the ac currents flowing in the same direction can be realized for the junctions transverse to the dc bias current. So far, the detailed study of the EW's dispersion in triangular Josephson ladders and arrays has not been carried out, as well as the study of the dependence of the resonant steps on the magnetic field. Thus in this paper we present measurements of the resonant steps in the current-voltage (I-V) characteristics of single and double row triangular Josephson arrays. For both systems, we calculate the spectrum of linear EW's and map it on the magnetic-field dependence of the step voltages. The paper is arranged as follows: in Sec. II our experimental observations are presented. In Sec. III, we introduce the model based on a set of equations, and derive the spectrum of linear EW's. Finally, Sec. IV contains a discussion of the obtained results and conclusions.

II. EXPERIMENTS WITH TRIANGULAR JOSEPHSON JUNCTION LADDERS AND ARRAYS

In order to investigate the dynamical behavior of triangular arrays in the presence of an external magnetic field, we have chosen linear arrays made of one row and two rows, as shown in Figs. 1(b) and (c). Arrays of various critical current densities and sizes of the elementary cells have been measured. The arrays were made of Nb/Al-AlO_x/Nb underdamped Josephson tunnel junctions, arranged in a triangular lattice. The junction area is designed to be 9 μm^2. The studied critical current densities are $j_c \approx 50$ A/cm^2 and $j_c \approx 1000$ A/cm^2. The junction capacitance C is about 300 and 450 pF, respectively. The bias current I_b is uniformly injected in each node of the array via on-chip resistors and extracted as shown by arrows in the sketches.[15] The voltage is measured in the direction along the bias, across each individual row. The measurements have been performed using the acquisition software of Ref. 16. Experiments have been performed in the presence of a magnetic field applied perpendicular to the cell plane. Following the standard notation, we express the magnetic field in terms of the frustration f. The self-inductance of one cell can be roughly estimated[17] as

$$L = 1.25\mu_0\sqrt{A}, \tag{2}$$

where μ_0 is the free space permeability, and A is the cell hole size. The value of L is needed for calculating the parameter $\beta_L = 2\pi L I_c/\Phi_0$, where I_c is the junction critical current. The value given by Eq. (2) underestimates the actual inductance of the cell, as it is an asymptotic value valid only when the width of the superconducting electrodes forming the cell is larger than the hole size.[17] On the contrary, our arrays are in the opposite limit. We have compared the calculated value [Eq. (2)] with the value $\tilde{L}$ obtained from the magnetic-field dependence of the critical current of a single cell with two junctions, i.e., a superconducting quantum interference device (SQUID). The ratio of the minimum to the maximum critical currents of the SQUID reflects the value of its β_L parameter[14] and therefore the value of the cell inductance.[19] The relation between the two values was found to be $L \approx 0.7\tilde{L}$. However, in order to make a systematic comparison of all studied arrays, the β_L values reported here refer to the cell inductance estimated from Eq. (2). To get various values of β_L, we have used samples either with different critical current densities and same cell size, or have varied the cell size A from 126 to 240 μm^2 for similar arrays located on one chip. Thus the parameter β_L varied between 0.5 and 5, at the temperature $T=4.2$ K. The investigated arrays and their parameters are summarized in Table I.

TABLE I. The arrays parameters at $T=4.2$ K.

Sample [a]	1	2	3	4	5	6
No. of rows	1	1	1	1	1	2
No. of cells per row	10	12	10	10	10	12
Cell area (μm^2)	126	160	126	180	240	160
j_c(A/cm^2)	30	1050	50	50	50	1050
β_L	0.5	5	1.6	1.9	2.2	5

[a]All the studied samples have three junctions per cell.

The measured I-V curves of the triangular ladders show well defined resonances, grouped in two different voltage regions. Figure 2(a) shows an enlargement of the I-V curve of a ten cell row with $\beta_L \approx 0.5$ at $f=0.3$. Here S_1 and S_2 denote the upper and lower voltage resonances, respectively. The steps of type S_1 and S_2 are stable in approximately the same range of frustration. Changes of f induce a periodic modulation of the voltages $V_{1,2}$ of the steps. In particular, S_1 and S_2 approach the maximum voltage at $f=0.5$ (and other half integer values), and tend to the minimum value of voltage at integer f. Figure 2(b) shows the $V_{1,2}(f)$ dependences

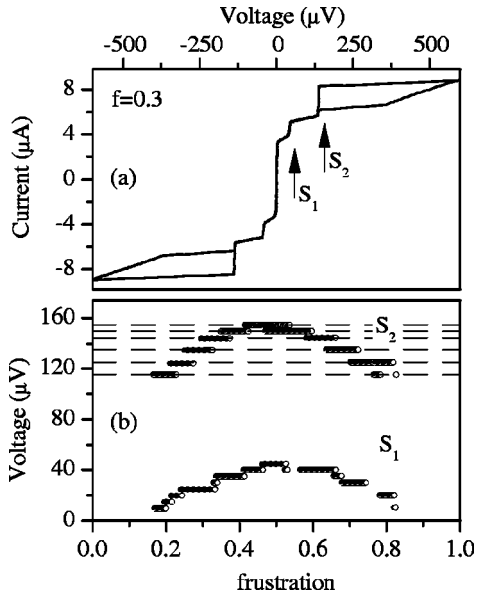

FIG. 2. (a) I-V characteristic of a one-row array at $f=0.3$; (b) step voltage dependences vs f of S_1 and S_2 (sample 1); dashed lines represent the well-defined resonances of the step S_2. Here $\beta_L=0.5$ and $T=4.2$ K.

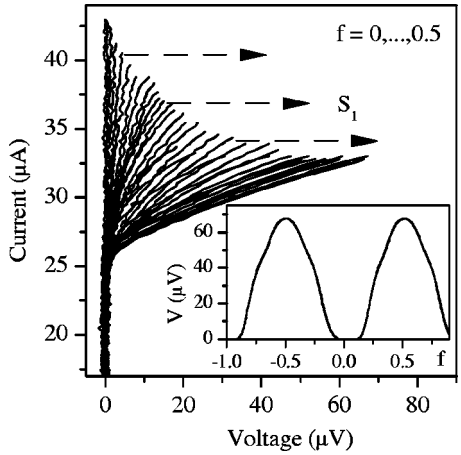

FIG. 3. Sequence of S_1 steps recorded while slowly changing f in the range 0–0.5. The single row array has 12 cells and a $\beta_L \approx 5$ (sample 2). Straight arrows indicate the transition from the step to the McCumber branch. Inset: the voltage across the array at the bias point $I_b \approx 32\mu$A is smoothly tuned from 0 to 65μV as f changes.

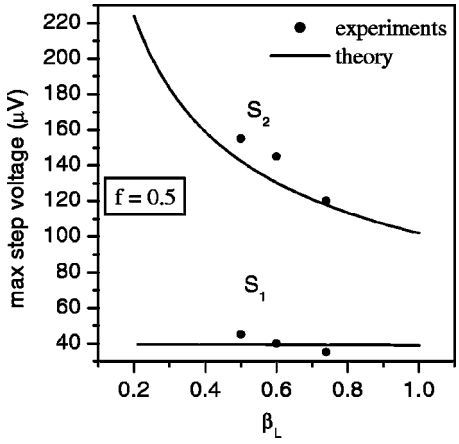

FIG. 4. Filled symbols: Maximum voltage of the steps S_1 and S_2 measured at $f=0.5$ in arrays having three different values of cell inductance L (samples 3, 4, 5). These arrays have ten cells, $j_c \approx 50$ A/cm^2 and $\omega_p \approx 7$ GHz. Solid lines are the theoretical prediction [Eq. (9)] for the upper and lower resonances, for $q=0.5$.

in the range $0 \leqslant f \leqslant 1$. The step S_2 has a typical resonant behavior. It clearly shows distinctly different voltages [underlined by the dashed lines of Fig. 2(b)] that correspond to the minima of the differential resistance on the step. However, we have noticed that the resonant regime of the step S_2 is realized only in the case of low β_L, i.e., for small discreteness. In arrays with either larger I_c or larger L (both these quantities lead to an increase of β_L) the resonant behavior disappears and the step S_2 changes continuously with f.

The voltage and the differential resistance of the step S_1 have almost a continuous dependence on f for all the investigated β_L parameters. In general, the differential resistance of the step S_1 is higher than that of S_2. This feature is enhanced in the samples with large β_L, as Fig. 3 shows for the case of a single row array of 12 cells and $\beta_L \approx 5$. At a constant bias current chosen on the step S_1, by changing f we could continuously tune the voltage across the array, along the periodic pattern shown in the figure inset.

The maximum voltage of the steps S_1 and S_2, i.e., the voltage value approached at $f=0.5$, depends on the cell inductance. We have compared the maximum voltages of three triangular ladders (samples 3, 4, 5) designed with different cell sizes ($A=126$, 180, and 240μm^2, respectively) and same junction area, and fabricated with the same critical current density ($j_c \approx 50$A/cm^2). The data reported in Fig. 4 show a tendency for the maximum voltages of both S_1 and S_2 to decrease as the β_L (cell size) increases. Both the experimental and theoretical curves show that this effect is more pronounced for the step S_2 than for the step S_1. Increasing temperature also leads to a reduction of the maximum step voltages, similarly to the results reported in Ref.4.

In experiments with two row arrays [Fig. 1(c)], we have used a common bias current for both rows, and have independently measured the voltage across each of them. Figure 5 shows the typical I-V characteristics of an array made of 12(cells)$\times$2(rows), sample 6. Both rows (denoted as A and B) have very similar I-V curves. At the same critical current, the rows switch simultaneously to the finite voltage state, with the same voltage. Similar to the case of single row arrays, in the presence of frustration we distinguish the steps S_1 and S_2. In Fig. 5 these steps are plotted at $f=0.4$. No hysteresis is observed in this case. The steps are found to be periodically modulated by the magnetic field, in a similar way as it is described above for the single row array. Moreover, their maximum voltages approached at $f=0.5$ are similar to that observed in the single row array with the same discreteness parameter (sample 2), i.e., with the same cell size ($A=160\mu$ m^2) and critical current density ($j_c = 1050$A/cm^2). The interesting feature observed in the two row arrays is the presence of a third step, marked as S_3 in Fig. 5. The peculiarity of this resonance is that it is stable at frustration values corresponding to an integer number of fluxons per cell ($f=0,\pm 1,\ldots$). At these values of f, an in-

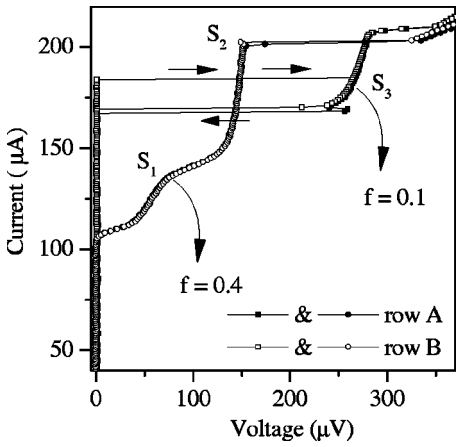

FIG. 5. I-V characteristics for the two row array showing the steps S_1 and S_2 at $f=0.4$ (open and filled circles), and the extra step S_3 at $f=0.1$ (open and filled squares). Data refer to the voltages measured independently across the individual rows, noted as A and B. Straight arrows indicate the hysteretic path. Sample 6, $\beta_L=5$.

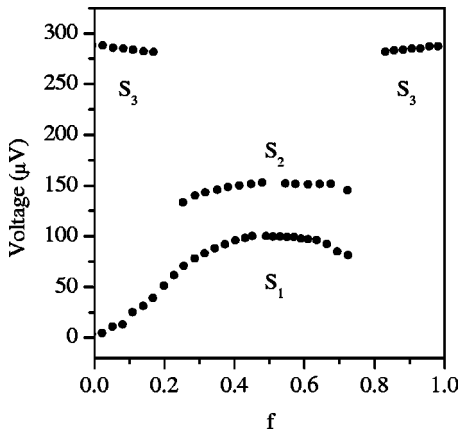

FIG. 6. Measured dependences of the maximum voltages of the steps S_1, S_2, and S_3 as a function of frustration for the two row array (sample 6). Data refer to the voltage measured across one row (A), another row (B) exhibited simultaneously the same voltage state.

crease of I_b above the array critical current induces both rows to jump simultaneously to the state S_3. Further increasing of I_b causes the transition from S_3 to the McCumber branch. The I-V curve is hysteretic and a decrease of I_b along S_3 eventually reaches an instability point with a certain retrapping current, at which the array returns to the zero voltage state. Sometimes, by decreasing I_b, at the instability point the two rows split and while one row goes to $V=0$, the other row undergoes a transition to higher voltages and then to $V=0$, with a slightly lower retrapping current (this behavior is shown in Fig. 5).

The dependences of the maximum voltages of the steps S_1, S_2, and S_3 on f are shown in Fig. 6. In contrast to S_1 and S_2, the step S_3 moves to lower voltages when approaching $f=0.5$. We note that the voltage modulation is more pronounced for the steps S_1 and S_2 than for S_3. Moreover, increasing the temperature above 4.2 K causes only a slight reduction of the step voltage. Above $f\approx 0.2$ the step S_3 disappears and the steps S_1 and S_2 become stable. Although not shown in the figure, the step S_1 is stable in the entire frustration range $f=0,\ldots,1$.

III. MODEL AND SPECTRUM OF LINEAR ELECTROMAGNETIC WAVES

The derivation of the equations of motion for a triangular array is done in a way similar to the case of one-dimensional (1D) arrays (two junctions per cell)[4] and ladders (four junctions per cell).[3,12] The junctions are described by the resistively and capacitively shunted junction (RCSJ) model.[14] We neglect mutual inductances and consider only the self inductances of the cells. We denote with $\varphi_{i,j}$ and $\varphi_{i+1,j}$, respectively, the superconducting phase differences (Josephson phases) across the *vertical* junctions of the cell i in the row j ($j=1,2$) and with $\psi_{i,k}$ the phase differences across the *horizontal* junction of the cell i in the line k ($k=1,2,3$). For the one-row case the indexes j and k are unnecessary and therefore omitted. With Φ_i and $\Phi_{\rm ext}$ we denote the induced and the applied magnetic flux, respectively. First, we derive the equations of motion for the ''triangular'' Josephson ladder of Fig. 1(b). We recall the fluxoid quantization in the cell i:

$$\varphi_{i+1}-\varphi_i+\psi_i=-\frac{2\pi\Phi_i}{\Phi_0}. \tag{3}$$

Due to nonzero cell inductance L, Φ_i, and $\Phi_{\rm ext}$ are related by

$$\Phi_i=\Phi_{\rm ext}+LI_i, \tag{4}$$

where I_i is the mesh current in the cell i. By making use of Kirchhoff's current law, we get

$$C\dot{V}_i^v+\frac{V_i^v}{R}+I_c\sin\varphi_i=I_b-I_i+I_{i-1}, \tag{5}$$

where V_i^v is the voltage across the vertical junction i. All junctions have capacitance C, resistance R, and critical current I_c. Since the current flowing through the horizontal branch is the mesh current I_i, for the horizontal junctions we obtain

$$C\dot{V}_i^h+\frac{V_i^h}{R}+I_c\sin\psi_i=I_i. \tag{6}$$

Finally, the equations of motion for the vertical and horizontal junctions of the row read as

$$\ddot{\varphi}_i+\alpha\dot{\varphi}_i+\sin\varphi_i=\gamma+\frac{1}{\beta_L}(\varphi_{i+1}-2\varphi_i+\varphi_{i-1}+\psi_i+\psi_{i-1})$$

$$\ddot{\psi}_i+\alpha\dot{\psi}_i+\sin\psi_i=\frac{1}{\beta_L}(\varphi_i-\varphi_{i+1}-\psi_i)-\frac{2\pi f}{\beta_L}. \tag{7}$$

Here, the time unit is $\omega_{\rm p}^{-1}=\sqrt{\hbar C/(2eI_c)}$, the inverse plasma frequency. The parameter $\alpha=1/\sqrt{\beta_c}$ determines the damping[14] of the junctions and the parameter β_L defines the discreteness of the array; f is the frustration defined above, and $\gamma=I_b/I_c$ is the normalized bias current.

To derive the spectrum of EW's, we assume a whirling solution along the vertical junctions and oscillations with a small amplitude for the horizontal junctions. Moreover, the phase of the vertical junctions increases from cell to cell due to the presence of frustration. Thus the solutions of Eqs. (7) can be written as

$$\varphi_n=\omega t+2\pi fn+\varphi e^{i(\omega t+2\pi qn)},$$

$$\psi_n=\psi e^{i(\omega t+2\pi qn)}, \tag{8}$$

where ω and q are, respectively, the angular frequency and the wave number of the EW in the array. In the limit of small amplitudes φ and ψ, we obtain the spectrum of electromagnetic wave propagating along the array. This spectrum consists of *two* branches $\omega_+(q)$ and $\omega_-(q)$ given by

$$\omega_\pm=\omega_p\sqrt{\mathcal{F}\pm\sqrt{\mathcal{F}^2-\mathcal{G}}}, \tag{9}$$

where $\mathcal{F}=1/2+1/(2\beta_L)+(2/\beta_L)\sin^2(\pi q)$, and $\mathcal{G}=(4/\beta_L)\sin^2(\pi q)$. The two modes are plotted in Fig. 7 for

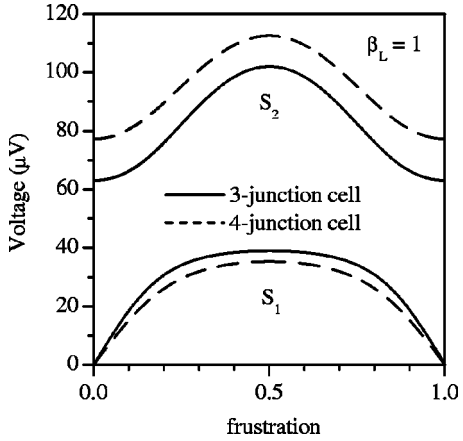

FIG. 7. The two linear modes in a single row array with three junctions per cell (continuous line) and four junctions per cell (dashed line). $\beta_L=1$.

the case $\beta_L=1$. This dispersion relation differs from that derived in Ref. 3 for the case of ''square'' Josephson ladders [four instead of three small junctions per elementary cell, Fig. 1(a)] only by a constant factor. The horizontal junctions play an essential role in the array dynamics, and lead to two linear resonances in the dispersion relation. If, instead of the horizontal junction, simply a superconducting link is placed, that is, the case of well-known 1D parallel array, only *one* linear mode exists.[1,2]

Thus what should we expect when two rows of cells join together in a 2D array? In order to describe the spectrum of linear modes in the two-row array, we use the time-dependent Josephson phases of vertical $\varphi_{i,j}(t)$ and $\varphi_{i+1,j}(t)$ and horizontal $\psi_{i,k}(t)$ junctions. Similar to the one row case, we derive the set of equations by means of the Kirchhoff's current law and the fluxoid quantization. Assuming a whirling solution along the vertical junctions and oscillations with a small amplitude for the horizontal junctions, we obtain the spectrum of linear modes from the system of seven linear equations:

$$
\begin{aligned}
-\beta_L\omega^2\varphi_{i,1}&=\varphi_{i+1,1}(1+e^{-iq})-2\varphi_{i,1}-\psi_{0,i+1}-\psi_{-1,i}e^{-iq},\\
-\beta_L\omega^2\varphi_{i+1,1}&=\varphi_{i,1}(1+e^{iq})-2\varphi_{i+1,1}+\psi_{-1,i}+\psi_{0,i+1},\\
-\beta_L\omega^2\varphi_{i,2}&=\varphi_{i+1,2}(1+e^{-iq})-2\varphi_{i,2}+\psi_{0,i+1}+\psi_{1,i}e^{-iq},\\
-\beta_L\omega^2\varphi_{i+1,2}&=\varphi_{i,2}(1+e^{iq})-2\varphi_{i+1,2}-\psi_{0,i+1}-\psi_{1,i},\\
\beta_L(-\omega^2+1)\psi_{1,i}&=(\varphi_{i,2}e^{iq}-\varphi_{i+1,2}-\psi_{1,i}),\\
\beta_L(-\omega^2+1)\psi_{-1,i}&=(\varphi_{i,1}e^{iq}-\varphi_{i+1,1}-\psi_{-1,i}),\\
\left(-\omega^2+1+\frac{1}{\beta_L}\right)(\psi_{-1,i}+\psi_{1,i})&=\psi_{0,i+1}\frac{(1-\omega^2)(e^{iq}-1)}{\beta_L\omega^2}.
\end{aligned}
\tag{10}
$$

By solving the system of Eqs. (10), we obtain *seven* branches in the $\omega(q)$ dependence. Three branches are determined by the equation

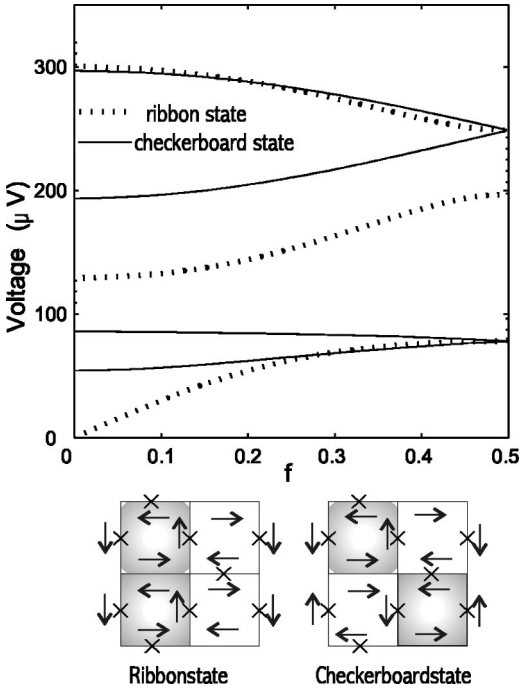

FIG. 8. Calculated spectrum for the linear modes in the two-row array and sketches of the ac mesh current distribution at $f=0.5$.

$$
\omega^6-\left(\frac{5}{\beta_L}+1\right)\omega^4+\left(\frac{4}{\beta_L}+\frac{6}{\beta_L^2}-\frac{4}{\beta_L^2}\cos^2\frac{q}{2}\right)\omega^2-\frac{4}{\beta_L^2}\sin^2\frac{q}{2}=0. \tag{11}
$$

These branches correspond to a *ribbon* state,[7] as the Josephson junctions of the middle row are not active ($\psi_0=0$). The lower ribbon branches displays an $\omega(q)$ dependence which increases as the wave vector increases. As observed in the experiments, the upper branch displays a different behavior with respect to the lower branches, i.e., ω increases as the wave vector decreases (alternatively, the voltage increases as the frustration decreases).

The other four solutions of the system of Eqs. (10) involve oscillations of the junctions in the middle row and therefore correspond to a *checkerboard* state (at $f=0.5$). These four branches are determined by the equation

$$
\left[\left(-\omega^2+\frac{2}{\beta_L}\right)\beta_L^2\left(1-\omega^2+\frac{1}{\beta_L}\right)-2\right]\times\left[-2\omega^2+\left(\frac{2}{\beta_L}-\omega^2\right)(1-\omega^2)\right]=2(1-\omega^2)^2\cos^2\frac{q}{2}. \tag{12}
$$

As in the ribbon case, the upper branch of the checkerboard state has a different dependence on f with respect to the lower checkerboard branches. All the linear modes calculated for the double row array are plotted in Fig. 8. As one can see, the qualitative behavior of these linear modes is in a good agreement with the experimental data reported in Fig. 6. Thus the linear approximation used for modeling the dy-

namic behavior of the frustrated arrays is sufficient to quantitatively explain the most essential features observed in the experiments.

IV. DISCUSSION AND CONCLUSIONS

In the previous section we derived the spectrum $\omega(q)$ of EW's for triangular Josephson ladders and for double row arrays. In the Josephson ladder case [Fig. 1(b)], we obtain *two* branches $\omega_{\pm}(q)$ (Fig. 7). The excitation of the EWs that account for these branches leads to resonant steps in the I-V curves (Fig. 2). Although the current amplitude of the resonant steps depends on the array parameters in a rather complicated way, *the voltage positions* of the steps can be mapped to the spectrum of linear EW's by making use of the Eq. (1). Indeed, we obtain a good agreement between the magnetic-field (frustration f) dependence of the step voltages [Fig. 2(b)] and the calculated spectrum $\omega_{\pm}$ (Fig. 7). The dependence of the maximum voltages on the discreteness parameter β_L shown in Fig. 4, displays also a good agreement with the theoretical prediction. Thus the limiting operation voltage (i.e., frequency) for each mode can be controlled by the geometrical inductance and/or by the critical current density.

The calculated spectrum of EW's for the double row triangular Josephson array contains *seven* branches (Fig. 8). Three of them correspond to the ribbon state, while the others are due to the checkerboard state. However, the experimental data show that only three branches are excited in the Josephson arrays and, correspondingly, only three resonances appear in the current-voltage characteristics. The reason for this might be ascribed to internal instabilities of the states. The observed resonances S_1, S_2, and S_3 (Fig. 6) can be mapped to the spectrum of EW's (Fig. 8). Moreover, the observed peculiar resonance (S_3) appears at the small values of frustration f, and its voltage *decreases* with f. Two branches with the similar behavior are also found in the spectrum $\omega(q)$ of EW's (Fig. 8), one corresponding to the checkerboard and the other to the ribbon state. Unfortunately, measurements of I-V curves do not allow us to distinguish between these branches and, correspondingly, between the ribbon and checkerboard states. A distinction can be, in principle, done by detecting radiation from the array due to properly coupled ac voltage.

In conclusion, we have studied the dynamical states of triangular arrays of Josephson junctions in the presence of a magnetic field. As expected, the number of exhibited resonances increases with the number of degrees of freedom of the system. We found that in one-row arrays there are two states, and that in two-row arrays three states are observed. The proposed analytical model allows us to obtain the spectrum of linear modes, both for single and double row triangular arrays. The voltage position of the observed resonances is mapped to this spectrum and good agreement between experiments and theory is found.

ACKNOWLEDGMENTS

We thank Stanford Yukon and Giacomo Rotoli for valuable and stimulating discussions. We are grateful to Marcus Schuster for his critical reading of the manuscript. Samples were made in part at Research Center Juelich (FZJ) and in part at Hypres.[18] The European Office of Aerospace Research and Development (EOARD) and the Alexander von Humboldt Stiftung are acknowledged for supporting this work.

*On leave from Universitá degli studi di Salerno, Dipartimento di Fisica, Via. S. Allende, I-84081 Baronissi (Salerno), Italy.

†Permanent address: Max-Planck Institut für Physik Komplexer Systeme, Nöthnitzer Str. 38, D-01187 Dresden, Germany.

[1] H. S. J. van der Zant, T. P. Orlando, S. Watanabe, and S. H. Strogatz, Phys. Rev. Lett. **74**, 174 (1995).

[2] A. V. Ustinov, M. Cirillo, B. H. Larsen, V. A. Oboznov, P. Carelli, and G. Rotoli, Phys. Rev. B **51**, 3081 (1995).

[3] P. Caputo, M. V. Fistul, B. A. Malomed, S. Flach, and A. V. Ustinov, Phys. Rev. B **59**, 14 050 (1999).

[4] M. Barahona, E. Trías, T. P. Orlando, A. E. Duwel, H. S. J. van der Zant, S. Watanabe, and S. H. Strogatz, Phys. Rev. B **55**, 11 989 (1997).

[5] P. Binder, D. Abraimov, A. V. Ustinov, S. Flach, and Y. Zolotaryuk, Phys. Rev. Lett. **84**, 745 (2000); P. Binder, D. Abraimov, and A. V. Ustinov, Phys. Rev. E **62**, 2858 (2000).

[6] E. Trias, J. J. Mazo, and T. P. Orlando, Phys. Rev. Lett. **84**, 741 (2000).

[7] S. P. Yukon and N. C. Lin, in *Macroscopic Quantum Phenomena and Coherence in Superconducting Networks* (World Scientific, Singapore, 1995), p. 351; IEEE Trans. Appl. Supercond. **7**, 3115 (1997).

[8] P. Caputo, A. V. Ustinov, and S. P. Yukon, IEEE Trans. Appl. Supercond. (to be published).

[9] A. V. Ustinov, in *Lectures on Superconductivity in Networks and Mesoscopic Systems*, edited by C. Giovannella and C. J. Lambert, AIP Conf. Proc. No. **427** (AIP, Woodbury, NY, 1998), pp. 31-55.

[10] A. E. Duwel, E. Trias, T. P. Orlando, H. S. J. van der Zant, S. Watanabe, and S. Strogatz, J. Appl. Phys. **79**, 7864 (1996).

[11] C. De Leo and G. Rotoli, IEEE Trans. Appl. Supercond. (to be published); C. De Leo and G. Rotoli, presented at EURESCO conference, July 2000, Maratea, Italy–available online at http://www.ing.univaq.it/energeti/research/Fisica/posASC2000.pdf

[12] G. Grimaldi, G. Filatrella, S. Pace, and U. Gambardella, Phys. Lett. A **223**, 463 (1996).

[13] M. V. Fistul, P. Caputo, and A. V. Ustinov, Phys. Rev. B **60**, 13 152 (1999).

[14] A. Barone and G. Paternó, *Physics and Applications of the Josephson Effect* (Wiley, New York, 1982).

[15] The model of square cells with three Josephson junctions per cell is equivalent to the triangular lattice, as in the triangular geometry the bias current injected in the inner vertical branches is twice as large as the current injected in the outermost branches.

This is because a square cell is transformed in a triangular cell by joining two adjacent nodes.

[16] GoldExi for Windows, http://www.geocities.com/goldexi/

[17] J. M. Jaycox and M. B. Ketchen, IEEE Trans. Magn. **MAG.-17**, 400 (1981).

[18] HYPRES Inc., Elmsfort, NY 10523.

[19] The measured I_c vs f dependences for the single cell with two junctions and the single cell with three junctions did not reveal substantial differences, as expected in the large inductance limit.